Soft Matter

RSC Publishing

PAPER

View Article Online
View Journal | View Issue

Cite this: *Soft Matter*, 2013, **9**, 4655

Ethanol promotes dewetting transition at low concentrations

Xiuping Ren,[ab] Chunlei Wang,[a] Bo Zhou,[ab] Haiping Fang,*[a] Jun Hu*[a] and Ruhong Zhou*[cd]

Received 7th January 2013
Accepted 5th March 2013

DOI: 10.1039/c3sm00049d

www.rsc.org/softmatter

Recent studies have suggested important roles for nanoscale dewetting in the stability and self-assembly dynamics of both physical and biological systems. Less known is the cosolvent (such as ethanol) effect on nanoscale dewetting. Here, we use molecular dynamics simulations to investigate the dewetting behavior in-between two hydrophobic plates immersed in ethanol aqueous solutions, particularly at low concentrations. Unexpectedly, the existence of a small amount of ethanol molecules promotes the dewetting transition in the inter-plate region at a greater separation that is otherwise non-existent in pure water or pure ethanol. We find that a competition for ethanol molecules at equilibrium among the inter-plate region, the outer-surfaces of the plates and the bulk solution results in a depletion of ethanol molecules in the inter-plate region. Meanwhile, the preferred inward orientations of the ethanol ethyl groups at the liquid–vapor interface located at the edge of the plates make the inter-plate core more hydrophobic so that water molecules are more favored to be expelled, thus resulting in an enhancement of the dewetting. These findings provide a deeper understanding of the effects of cosolvents on the hydrophobic interaction.

1 Introduction

Alcohols, which have a non-polar tail and a polar head, are widely used as cosolvents in both chemical and biological fields. As a short-chain alcohol and a very common small organic compound, ethanol has many different roles, such as binding to the hydrophobic domains of pores, inhibiting recombinant *N*-methyl-D-aspartate receptors and blocking ion fluxes within channels thus causing behavioral disorders or anesthesia.[1–4] Despite the above significant roles of ethanol molecules in these nanoconfined pores/cavities, little is known experimentally about their molecular-scale behavior within those pores/cavities.

Recent investigations show that nanoscale dewetting, as an extreme case of hydrophobic interactions, can play an essential role in many chemical and biophysical processes, such as protein folding, ligand binding, ion channel gating and the self-assembly of amphiphiles into micelles and membranes.[5–11] Nanoscale dewetting here means that there exists a water dewetting transition when in some extreme cases the hydrophobic interaction is very strong, *i.e.* when water molecules trapped inside nanopores/nanocavities or in-between nano-distance-separated hydrophobic surfaces spontaneously evaporate.[12–26] Although ethanol aqueous solutions are abundant in chemical and biophysical systems, there is little study on the dewetting property of ethanol aqueous solutions. On the other hand, there have been some theoretical studies, including molecular dynamics (MD) simulations, focusing on the effects of hydrogen bonding on the structures of alcohol–water mixtures,[27–30] and the wetting of water[31] and water–ethanol droplets on a non-polar surface.[32] Since ethanol is a small amphiphilic molecule, one may expect that the existence of ethanol molecules in the dilute solution will degrade the dewetting behavior.

In this paper, we will show the unexpected promotion of the dewetting transitions in-between two hydrophobic plates (THPs) in ethanol aqueous solutions by using extensive MD simulations. We find that ethanol molecules prefer to accumulate at the liquid–vapor interface and that at low concentrations the competition for ethanol molecules among the inter-plate region, the outer-surfaces of the plates and the bulk solution results in insufficient ethanol molecules to fill the inter-plate region at equilibrium. Meanwhile, the preferred inward orientations of the ethanol ethyl groups at the liquid–vapor interface located at the edge of the plates make the inter-plate core more hydrophobic so that water molecules are more favored to be expelled, thus resulting in a surprising enhancement of the dewetting under low ethanol concentrations. Our observations might be helpful for the better understanding of the dewetting transitions with cosolvents at the nanoscale, which may have technological and biological implications, for

[a]*Shanghai Institute of Applied Physics, Chinese Academy of Sciences, P.O. Box 800-204, Shanghai 201800, China. E-mail: fanghaiping@sinap.ac.cn; hujun@sinap.ac.cn*

[b]*Graduate School of the Chinese Academy of Sciences, Beijing 100080, China*

[c]*IBM Thomas J. Watson Research Center, Yorktown Heights, NY 10598, USA. E-mail: ruhongz@us.ibm.com*

[d]*Department of Chemistry, Columbia University, New York, NY 10027, USA*

example, in novel designs of nano-devices such as molecular switches and gates.

2 Simulation methods

The MD package GROMACS version 3.3.3[33] was used for all simulations with a time step of 1 fs. The Lennard-Jones diameter and well depth of each particle were $\sigma_p = 0.4$ nm and $\varepsilon_p = 0.5$ kJ mol^{-1}, respectively. These parameters are the same with the model hydrophobic plates used in the previous work by Berne *et al.*[34] Parameters for ethanol molecules were taken from the all-atom OPLS (optimized potentials for liquid simulations) force field.[35] The rigid extended simple point charge water was used throughout[36] and the SETTLE algorithm was used to keep the O–H distance fixed at 1 Å and the H–O–H angle at 109.47°.[37] Geometric combining rules were applied to calculate the Lennard-Jones interactions between different particles: $\varepsilon_{ij} = (\varepsilon_{ii}\varepsilon_{jj})^{1/2}$ and $\sigma_{ij} = (\sigma_{ii}\sigma_{jj})^{1/2}$, where ε_{ii} and σ_{ii} are the parameters of atom i for the Lennard-Jones diameter and well depth, respectively. As listed in Table 1, all the 16 solution systems with different initial ethanol concentrations of 0%, 0.25%, 0.5%, 1%, 2%, 3%, 4%, 5%, 8%, 10%, 12%, 15%, 18%, 20%, 25% and 100% (including 10026–12044 atoms) were first equilibrated at a constant pressure and temperature (NPT) of 1 bar and 298 K for 5 ns, after which the two plates were added to the simulation boxes (see Fig. 1(a)). Then, 15 ns NPT simulations were carried out after energy minimization with a steepest-descent algorithm. The NPT ensemble was maintained at a constant 298 K temperature using the Nosé–Hoover thermostat[38] and 1 bar pressure using the Parrinello–Rahman barostat.[39] The particle-mesh Ewald method[40] was used to treat long-range electrostatic interactions, and van der Waals interactions were treated with a cutoff distance of 1.2 nm.

3 Results and discussion

The model system with two parallel hydrophobic plates immersed in the ethanol aqueous solution is shown in Fig. 1(a). Each square plate with the size of 2.32×2.32 nm^2 was modeled as a single-layer of 49 neutral Lennard-Jones particles, which were arranged in a square lattice with a nearest-neighbor spacing of 0.32 nm. We have prepared 16 solution systems with different ethanol concentrations of 0%, 0.25%, 0.5%, 1%, 2%, 3%, 4%, 5%, 8%, 10%, 12%, 15%, 18%, 20%, 25% and 100%, respectively. The two plates were constrained with a harmonic potential ($k = 9000$ kJ mol^{-1} Å^{-2}) at initial inter-plate separations from 0.7 to 1.5 nm. Cubic periodic simulation boxes were used with side lengths from 4.8 to 5.1 nm. We allowed the first 5 ns of simulation time for system equilibration, and the subsequent 10–25 ns for data collection (even longer simulations, up to 100 ns, were collected and the results were basically the same, indicating that the nanoscale dewetting process is very fast).

Fig. 1(b) shows the atom number of the ethanol and water molecules located between the THPs as a function of the plate separation for four different systems (pure water, 5% ethanol, 10% ethanol and pure ethanol). For convenience, the atom numbers of the inter-plate ethanol and water molecules are denoted by $N_{ethanol}$ and N_{water}, respectively. For the pure water system, N_{water} increases very slowly as D increases from 0.7 nm, it jumps to the large value of ~370 at $D = 1.2$ nm and then continues to increase gradually. The small value of N_{water} at $D <$ 1.2 nm indicates that a vapor phase is dominant between the THPs, as shown by the typical snapshot in Fig. 1(d), consistent with the previous observations that a dewetting transition happens with an increased confinement of the liquid phase between plates.[13,15,41] In contrast, at $D = 1.2$ nm and beyond, water forms a dense liquid (Fig. 1(e)).

$N_{ethanol}$ for the pure ethanol system increases much faster than N_{water} for the pure water system. There is a small plateau at $D = 0.8$–1.1 nm with one layer of ethanol molecules filling the inter-plate region, as shown in Fig. 1(f). This result is in agreement with the observation that ethanol molecules wet hydrophobic solid surfaces more easily than water.[32] After the plateau, $N_{ethanol}$ increases again. Ethanol also forms a dense liquid at $D = 1.2$ nm (see Fig. 1(g)).

Table 1 Number of ethanol and water molecules for each system

System	Initial concentration	Ethanol	Water	Total atoms
Pure water system	0%	0	3982	11 946
	0.25%	4	3965	12 029
	0.5%	8	3938	11 984
	1%	16	3917	11 993
	2%	32	3851	11 939
	3%	48	3814	11 972
	4%	64	3790	12 044
5% ethanol system	5%	72	3496	11 136
	8%	114	3350	11 174
10% ethanol system	10%	138	3174	10 764
	12%	168	3149	11 057
	15%	216	3128	11 328
	18%	252	2933	11 165
	20%	270	2760	10 710
	25%	350	2624	11 022
Pure ethanol system	100%	1114	0	10 026

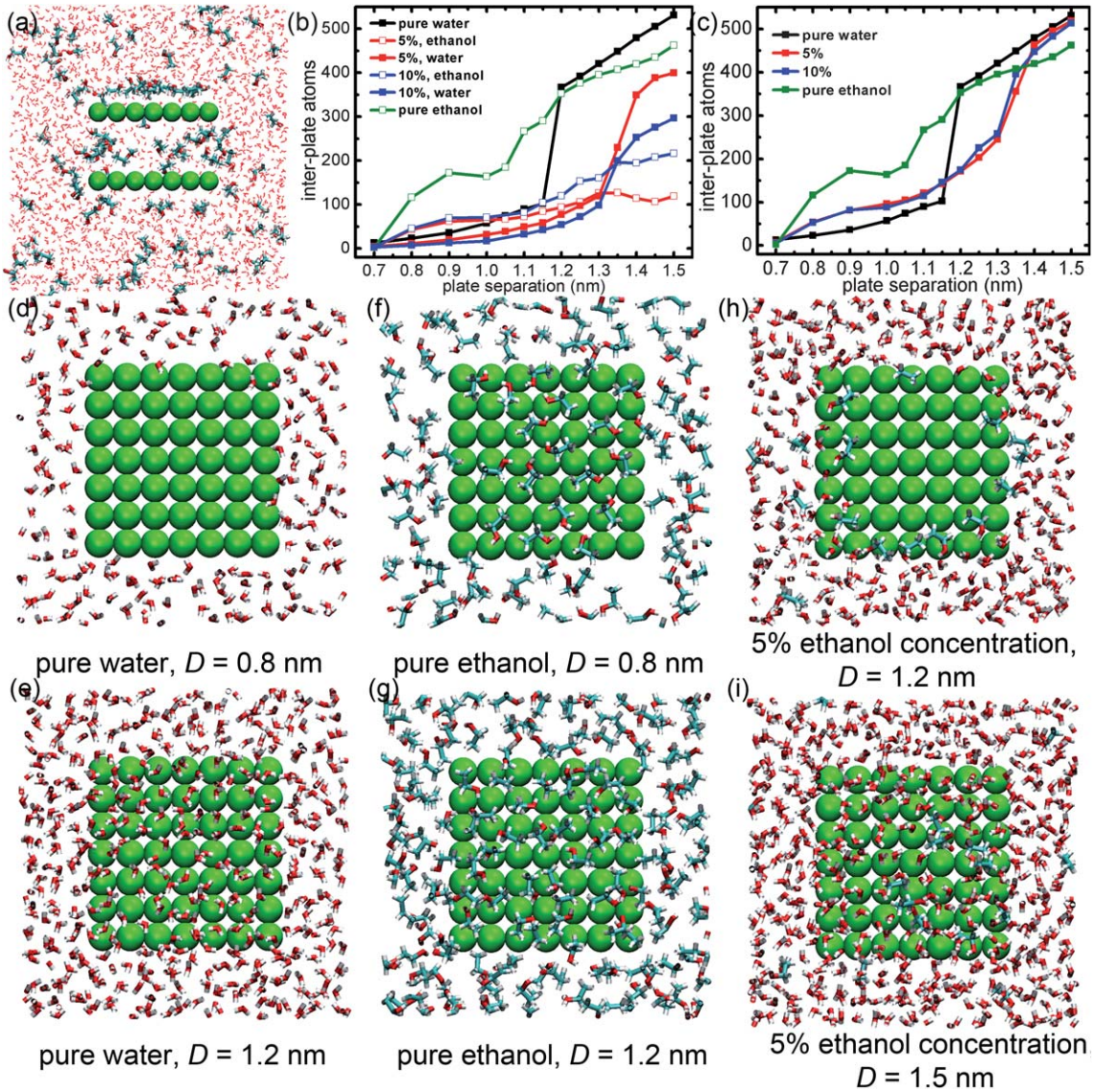

Fig. 1 (a) Snapshot of the simulation system. (b) and (c) numbers of the inter-plate water atoms (b, solid squares), ethanol atoms (b, open squares) and total atoms (c, solid squares) as a function of the plate separation for the pure water system (black), the 5% ethanol system (red), the 10% ethanol system (blue) and the pure ethanol system (olive), respectively. (d–i) Six typical snapshots of the simulation systems: (d) pure water system at $D = 0.8$ nm; (e) pure water system at $D = 1.2$ nm; (f) pure ethanol system at $D = 0.8$ nm; (g) pure ethanol system at $D = 1.2$ nm; (h) 5% ethanol system at $D = 1.2$ nm; (i) 5% ethanol system at $D = 1.5$ nm. The Lennard-Jones particles are depicted in green; water molecules are represented by red lines; carbon atoms, oxygen atoms and hydrogen atoms of each ethanol molecule are colored with cyan, red and white, respectively.

Fig. 1(c) shows the total atom number of the ethanol and water molecules located between the THPs as a function of the plate separation for four different systems (pure water, 5% ethanol, 10% ethanol and pure ethanol). For the two systems with 5% and 10% ethanol concentrations, interestingly, the total number of inter-plate ethanol and water atoms (N_{water} + $N_{ethanol}$) is still quite small at $D = 1.2$ nm. As shown in Fig. 1(h), there is still a vapor phase between the THPs at $D = 1.2$ nm, indicating that both water and ethanol are unable to fill the inter-plate region completely. This is unexpected since water or ethanol completely fills the inter-plate space at $D = 1.2$ nm for both the pure water and pure ethanol systems. It seems that the addition of ethanol promotes the water dewetting transition at a greater separation that is otherwise non-existent in pure water or pure ethanol.

In order to better characterize the wetting and dewetting behavior, we computed the critical dewetting distance, denoted by D_C, below which there is a stable vapor phase between the THPs.[6,7,24,25] In our study, we name a stable vapor phase between the THPs if the inter-plate atom density (N_{water} + $N_{ethanol}$)/($D_{effective} \times L^2$) is below 60% of the inter-plate atom density of the liquid state (defined as the density at $D = 1.5$ nm). Here, $D_{effective} = (D - 0.3)$ nm is the effective inter-plate distance, and L is the side length of 2.32 nm. The results are shown in Fig. 2. D_C initially increases almost monotonically with the ethanol concentration, P. D_C reaches 1.35 nm for the ethanol aqueous

solutions of 4%, 5%, 8% and 10%, which is much larger than $D_C = 1.2$ nm for the pure water system. Only very small changes in the D_C value are observed from $P = 4\%$ to 10% due to the finite size of the water molecules, and so do from 1% to 2%, from 12% to 15% and from 18% to 20%. D_C then decreases gradually from $P = 10\%$, and reaches the critical dewetting distance of 1.2 nm in pure water at $P = 25\%$. This shows that the dewetting-promoting effect only exists at low ethanol concentrations.

Now let us focus on the underlying physics. Since D_C from 1.2 to 1.35 nm is significantly larger than the $D = 0.8$ nm needed for ethanol molecules to fill the space in pure ethanol (comparing Fig. 1(h) with Fig. 1(f)), one might wonder why not enough ethanol molecules move into the inter-plate region to occupy the open space. In any multiphase system, the equal chemical potentials determine the number of molecules in different regions. In this case, we start our simulations with a uniform ethanol concentration everywhere, which is obviously a non-equilibrium system due to the nanoscale confinement of the THPs. It is the MD simulation that brings the system from a non-equilibrium state to an equilibrium one. During this process, ethanol molecules move from higher chemical potentials to lower ones. In general, the chemical potential for introducing an extra ethanol molecule inside the THPs should have a higher value due to the nanoscale confinement. Thus, it is unfavorable to accumulate more ethanol molecules inside the THPs during the competition for ethanol among various regions: in the bulk solution, on the outer surfaces of the THPs and in-between the THPs. Even as the initial ethanol concentration increases, there are indeed more ethanol molecules accumulating near the outer and inner surfaces of the THPs, but the inner THPs region is still less preferred due to its nano-confinement. As shown in Fig. 3, the number of ethanol molecules inside the THPs at equilibrium is below the linear fitting-line if a uniform concentration is assumed from higher concentrations. Therefore, ethanol molecules in the bulk cannot freely move into the inter-plate region to occupy the open space even if more ethanol molecules are available in the bulk.

This can also be understood from another view point. We note that the adsorption potentials (similar to chemical potential) are different for ethanol molecules adsorbed at different positions in-between the THPs. Assuming all ethanol molecules are in the bulk initially (non-equilibrium again), the ethanol molecules will be adsorbed into positions inside the THPs with the lowest adsorption potentials first, and then to positions with higher adsorption potentials. It is clear that the final equilibrium concentration of the ethanol molecules in the bulk solution and their average chemical potential determine how many ethanol molecules can move into the confined space, with the last ethanol molecule in the inter-plate region sharing the same chemical potential (or the highest adsorption potential). *Vice versa*, one can also conclude that the larger the number of ethanol molecules in-between the THPs is, the larger the equilibrium concentration of ethanol in solution is, as clearly seen in Fig. 3 where $N_{ethanol}$ increases with the equilibrium concentration of ethanol for all systems. Consequently, at too low concentrations, the space between the THPs cannot be completely filled by ethanol molecules, *i.e.* there is a depletion of ethanol molecules inside the THPs, although there are many in the bulk solution, due to the higher chemical potentials for the introduction of extra ethanol molecules in the confined space.

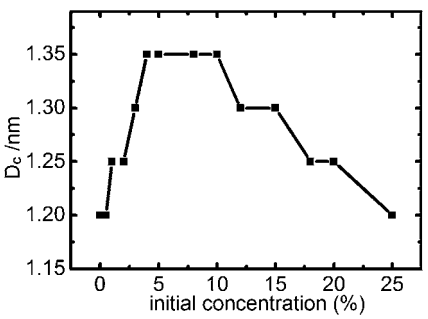

Fig. 2 Critical dewetting distance *versus* the initial concentration of ethanol.

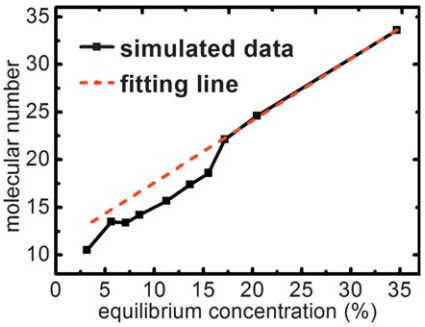

Fig. 3 Number of ethanol molecules between the THPs *versus* the equilibrium concentration of the bulk solution at $D = 1.2$ nm. The equilibrium concentration here is the ethanol concentration in the aqueous solutions after the system reached equilibrium. The dashed line is the fitting-line for the number of ethanol molecules inside the THPs if a uniform concentration is assumed from higher concentrations, indicating that at lower concentrations ethanol molecules are less favored inside the THPs region due to the nano-confinement.

Then, why are water molecules more favored to be expelled from the inter-plate region at low ethanol concentrations, *i.e.* why does the critical distance increase? As shown in Fig. 1(h), we can see that ethanol prefers to stay at the liquid–vapor interface located at the edge of the THPs. Moreover, those ethanol molecules have preferred orientations with the $-C_2H_5$ groups pointing inward and the –OH groups pointing outward of the inter-plate core. This can be seen more clearly in Fig. 4. There is a clear 'ethanol belt' at the liquid–vapor interface (see Fig. 4(a)) with preferred orientations with the ethanol $-C_2H_5$ groups pointing inward and –OH groups pointing outward of the inter-plate core (see Fig. 4(c)). This 'ethanol belt' together with the orientation configuration makes it more difficult for the water molecules to stay in the inter-plate core since the hydrophobic $-C_2H_5$ groups make the inner core between the THPs more hydrophobic, resulting in a lower mass density distribution of water at the inner core, as shown in Fig. 4(b). However, at too high ethanol concentrations (such as 20%), the

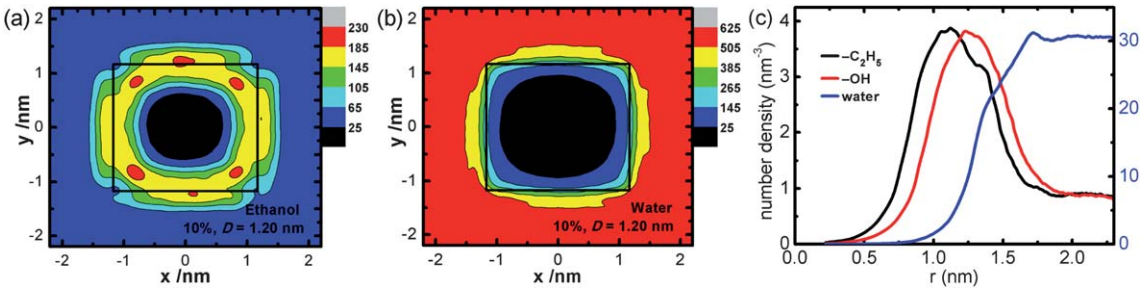

Fig. 4 Planar mass density distribution of ethanol (a) and water (b) at $D = 1.20$ nm for the 10% ethanol system in the x–y plane with z-coordinate between the THPs (unit nm^{-3}). The black solid lines represent the edge of the THPs. (c) Number density profiles of ethanol $–C_2H_5$, ethanol –OH, and water for the same system as (a) and (b), centering on the original point of (a) and (b).

extra ethanol molecules will disrupt the orientations of the ethanol molecules at the "ethanol belt" and thus weaken the hydrophobicity of the inner core between the THPs, which indicates that there will be a maximum critical distance – in this particular case with specified dimensions it is approximately 1.35 nm.

It should be pointed out that Lundgren *et al.* found that the contact angle decreased when ethanol molecules were present in water droplets on a non-polar surface,[32] implying a decrease of the critical dewetting distance from the theory, since $D_C \propto -\cos\theta_C$[13,41] ($\theta_C$ is the water contact angle, and $\theta_C > 90°$), or the disappearance of the dewetting transition ($\theta_C < 90°$). Interestingly, Balazs and coworkers have found that the contact angle between the fluid and the walls of microchannels decreases with the increase of the number of nanoparticles at the interface of binary fluids.[26] Our results indicate that the microscopic theory, $D_C \propto -\cos\theta_C$, might fail in predicting the critical dewetting distance in the presence of ethanol as a cosolvent at certain concentrations.

4 Conclusions

In this study, we employed molecular dynamics (MD) simulations of two hydrophobic plates (THPs) immersed in ethanol aqueous solutions to study the dewetting transition. We observe that the addition of a small amount of ethanol to water promotes the dewetting transition; this is unexpected and counter-intuitive. Our analyses show that ethanol molecules prefer to be adsorbed at the liquid–vapor interfaces. The number of ethanol molecules adsorbed in the nanoscale confined space depends on the equilibrium concentration of the bulk ethanol aqueous solution. The competition for ethanol molecules among different regions, in-between the THPs, the outer surfaces of the THPs and in the bulk solution, results in a depletion of ethanol molecules in the inter-plate region due to their nano-confinement induced higher chemical potential for extra ethanol molecules. Meanwhile, the specific orientations of the ethanol molecules at the liquid–vapor interface make the hydrophobic inter-plate core more hydrophobic due to the existence of ethyl groups. Our observations provide a deeper understanding of the dewetting behavior in cosolvent solutions under nanoscale confinement, including those in nanodevices and biosystems.

Acknowledgements

We thank Drs Wenpeng Qi, Guanghong Zuo and Peng Xiu for their constructive suggestions and helpful discussions. This work was supported by grants from the Chinese Academy of Sciences, and the National Science Foundation of China under grant nos. 10674146, 11204341 and 10825520, the National Basic Research Program of China under grant nos. 2007CB936000 and 2006CB933000, and the Shanghai Supercomputer Center of China. R.Z. acknowledges the financial support from the IBM Blue Gene Program.

References

1 Q. Zhou and S. A. Forman, *Biochemistry*, 2000, **39**, 14920–14926.
2 H. Ren, Y. Honse and R. W. Peoples, *J. Biol. Chem.*, 2003, **278**, 48815–48820.
3 Q. Shao, L. Huang, J. Zhou, L. Lu, L. Zhang, X. Lu, S. Jiang, K. E. Gubbins, Y. Zhu and W. Shen, *J. Phys. Chem. C*, 2007, **111**, 15677–15685.
4 M. Xu, L. J. Chandler and J. J. Woodward, *Alcohol*, 2008, **42**, 425–432.
5 B. J. Berne, J. D. Weeks and R. H. Zhou, *Annu. Rev. Phys. Chem.*, 2009, **60**, 85–103.
6 P. Ball, *Chem. Rev.*, 2008, **108**, 74–108.
7 R. Z. Wan, J. Hu and H. P. Fang, *Sci. China, Ser. G: Phys., Mech. Astron.*, 2012, **55**, 751–756.
8 C. Schäffer, A. M. Todea, H. Bögge, O. A. Petina, D. Rehder, E. T. K. Haupt and A. Müller, *Chem.–Eur. J.*, 2011, **17**, 9634–9639.
9 Z. Yang, B. Shi, H. Lu, P. Xiu and R. Zhou, *J. Phys. Chem. B*, 2011, **115**, 11137–11144.
10 L. H. Xie and M. P. Suh, *Chem.–Eur. J.*, 2011, **17**, 13653–13656.
11 S. Matysiak, P. G. Debenedetti and P. J. Rossky, *J. Phys. Chem. B*, 2012, **116**, 8095–8104.
12 F. H. Stillinger, *J. Solution Chem.*, 1973, **2**, 141–158.
13 K. Lum and A. Luzar, *Phys. Rev. E: Stat. Phys., Plasmas, Fluids, Relat. Interdiscip. Top.*, 1997, **56**, R6283–R6286.
14 Y. K. Cheng and P. J. Rossky, *Nature*, 1998, **392**, 696–699.
15 K. Lum, D. Chandler and J. D. Weeks, *J. Phys. Chem. B*, 1999, **103**, 4570–4577.

16 G. Hummer, S. Garde, A. E. Garcia and L. R. Pratt, *Chem. Phys.*, 2000, **258**, 349–370.
17 M. S. P. Sansom and P. C. Biggin, *Nature*, 2001, **414**, 156–158.
18 G. Hummer, J. C. Rasaiah and J. P. Noworyta, *Nature*, 2001, **414**, 188–190.
19 A. Wallqvist and B. J. Berne, *J. Phys. Chem.*, 2002, **99**, 2893–2899.
20 K. Leung, A. Luzar and D. Bratko, *Phys. Rev. Lett.*, 2003, **90**, 065502.
21 J. Y. Li, T. Liu, X. Li, L. Ye, H. J. Chen, H. P. Fang, Z. H. Wu and R. H. Zhou, *J. Phys. Chem. B*, 2005, **109**, 13639–13648.
22 N. Choudhury and B. M. Pettitt, *J. Am. Chem. Soc.*, 2005, **127**, 3556–3567.
23 X. Li, J. Y. Li, M. Eleftheriou and R. H. Zhou, *J. Am. Chem. Soc.*, 2006, **128**, 12439–12447.
24 S. Granick and S. C. Bae, *Science*, 2008, **322**, 1477–1478.
25 J. C. Rasaiah, S. Garde and G. Hummer, *Annu. Rev. Phys. Chem.*, 2008, **59**, 713–740.
26 Y. Ma, A. Bhattacharya, O. Kuksenok, D. Perchak and A. C. Balazs, *Langmuir*, 2012, **28**, 11410–11421.
27 N. Nishi, S. Takahashi, M. Matsumoto, A. Tanaka, K. Muraya, T. Takamuku and T. Yamaguchi, *J. Phys. Chem.*, 1995, **99**, 462–468.
28 S. J. Suresh and V. M. Naik, *J. Chem. Phys.*, 2002, **116**, 4212–4220.
29 Y. Andoh and K. Yasuoka, *J. Phys. Chem. B*, 2006, **110**, 23264–23273.
30 L. Yang and Y. Q. Gao, *J. Am. Chem. Soc.*, 2010, **132**, 842–848.
31 C. Wang, B. Zhou, Y. Tu, M. Duan, P. Xiu, J. Li and H. Fang, *Sci. Rep.*, 2012, **2**, 358.
32 M. Lundgren, N. L. Allan and T. Cosgrove, *Langmuir*, 2002, **18**, 10462–10466.
33 E. Lindahl, B. Hess and D. van der Spoel, *J. Mol. Model.*, 2001, **7**, 306–317.
34 R. Zangi, R. H. Zhou and B. J. Berne, *J. Am. Chem. Soc.*, 2009, **131**, 1535–1541.
35 W. L. Jorgensen, D. S. Maxwell and J. TiradoRives, *J. Am. Chem. Soc.*, 1996, **118**, 11225–11236.
36 H. J. C. Berendsen, J. R. Grigera and T. P. Straatsma, *J. Phys. Chem.*, 1987, **91**, 6269–6271.
37 S. Miyamoto and P. A. Kollman, *J. Comput. Chem.*, 1992, **13**, 952–962.
38 N. Shuichi, *J. Chem. Phys.*, 1984, **81**, 511–519.
39 M. Parrinello and A. Rahman, *J. Appl. Phys.*, 1981, **52**, 7182–7190.
40 U. Essmann, L. Perera, M. L. Berkowitz, T. Darden, H. Lee and L. G. Pedersen, *J. Chem. Phys.*, 1995, **103**, 8577–8593.
41 X. Huang, C. J. Margulis and B. J. Berne, *Proc. Natl. Acad. Sci. U. S. A.*, 2003, **100**, 11953–11958.

